FINE STRUCTURE IN CaII K LINE

L. M. Punetha, Uttar Pradesh State Observatory, Naini Tal, India

Received 3 August 1973

CaII K line spectrograms were traced at various wavelengths along the slit and also along the dispersion at regular intervals. Statistical properties, root mean square variations, full width at half maxima, autocorrelation functions, power and coherence spectra of intensity variations and profile parameters are described and discussed. It is emphasized that the large scale feature contribution to the average profile, with particular reference to the coarse mottle structure, be properly taken into account in the multicomponent atmospheric models.

Тонкая структура К линии Са II

Спектрограммы этой линии промерялись по разрезам и по дисперсии на регулярных интервалах. Приводятся и обсуждаются статистические параметры, средние квадратические вариации, ширина на среднем уровне, автокорреляционные функции, спектральные характеристики (мощность и когерентность) вариаций интенсивности и параметров профилей. Подчеркивается, что крупномасштабное распределение по отношению к среднему профилю, связанное в частности с крупной зернистой структурой, учтено в многокомпонентной модели атмосферы.

Introduction

De Jager (1959), and Linsky and Avrett (1970) have given a comprehensive summary of the papers dealing with the solar structure seen in the H and K lines of Ca II. These features became of interest ever since Hale and Deslandres obtained spectroheliograms in these lines. Hale and Ellerman (1903) found that the quiet Sun is covered with bright coarse and fine mottles, with the finest having a size of 1 second of arc. Deslandres (1910) noted that the most prominent feature of these spectroheliograms is the coarse network.

This network has been found to correspond to the supergranulation boundaries (Simon and Leighton, 1964). Bright features in K_2 correspond to the regions of enhanced magnetic field (Babcock and Babcock, 1955; Leighton, 1959; Howard, 1959, 1962). The interpretation and calibration of these emission features' K_2-width in terms of Wilson-Bappu (1957) relation have been discussed by Pasachoff (1971), and Bappu and Sivaraman (1971).

Rogerson (1955) has made spatial power spectrum analysis of the features in K_{232} spectroheliograms. Visibility of these features varies within the K line as the wavelength of observation is changed. These features and their visibility changes can be directly seen in good definition spectrograms (McMath et al., 1956; Pasachoff, 1970; Wilson et al., 1972). In this paper we have studied the wavelength variation of some statistical properties of these features as observed in K-spectrograms.

Observations and Reduction

The observations are based on a set of three spectrograms taken by Dr. M. K. V. Bappu, at the center of the solar disk, at the Kitt Peak National Observatory, in IV order, with a slit of 100 μ (15 mA or 170 km) and 6 second exposure. Spatial relationship between the three spectra is unknown, but features in them do not tally.

These spectra were traced in a direction perpendicular to the dispersion, at a set of wavelengths in the K line, with a microphotometer aperture of 100 μ × × 100 μ (15 mA × 170 km). Traces were read at 170 km interval on the Sun, at 540 points (91 000 km) such that the reference wire line shadow remains aligned for all the traces. Another set of plates with smaller scale (5·5″/mm) were traced parallel to the dispersion at regular (440 km) interval to study the profile parameters.

Each trace was smoothened by a three point running mean, $\chi_i = \frac{1}{3}(\chi'_{i-1} + \chi'_i + \chi'_{i+1})$, to eliminate photographic, reading and linear interpolation noise of photometric calibration. A third order mean polynomial was then subtracted out to remove trend and instrumental effects.

For four wavelengths, situated at K_3-wing, K_2-peak, K_2-wing and K_1-minima, pairs of intensity (INTY) traces, obtained from the opposite wings of the line, were combined together to give sum (SUM) and difference (DIFF) of intensities.

Autocorrelation functions (ACF) and cross correlation functions for 6 pairs and their resulting power,

phase and coherence spectra were calculated in the usual fashion (see, e.g., Edmonds et al., 1965). Connes (1961) data window was used for apodization. The power spectra were corrected for the transmission properties, $G(f) = \frac{1}{9}[1 + 2\cos(2\pi f)]^2$, of the running mean filter.

Functions obtained for the three spectra were combined together wavelength-wise to give mean functions and their internal probable error as $(0{\cdot}6745/\sqrt{3}) \times$ RMS variation.

Results

Figure 1 (see Plate 1) shows the intensity variations along the slit at various wavelengths in the K line. Large amplitude intensity fluctuations are due to the coarse mottle and network features, and they are common to all the wavelengths, conforming to the deduction of Hale and Ellerman (1903); and Jensen and Orrall (1963) that they have a columnar structure. Differences regarding their red and violet amplitudes and lateral spectral shift in their peaks, corresponding to rotating spectral features (Pasachoff et al., 1968), are discernible. These mottles are visible at $\Delta\lambda = 2{\cdot}3$ Å, but their influence may not extend much beyond (Smith, 1960).

Small scale features ($\simeq$1000 km) are visible at all wavelengths and they are superposed over the coarse structure. They usually do not extend over wavelength range greater than 150–200 mA (Pasachoff, 1970).

Intensity distribution on each trace, as measured by the slit length covered at various intensity levels (Fig. 1), shows a symmetrical part, corresponding to bright and dark mottles (Jensen and Orrall, 1963) and an asymmetrical high intensity tail, corresponding to the overbright coarse network structure. This asymmetry is maximum at K_2 level.

Wavelength ($\Delta\lambda$) variation of the two gross parameters, Full Width at Half Maxima (FWHM) and Root Mean Square (RMS) variation, characterizing the second moment of distributions, are shown in Fig. 2.

The FWHM provides a measure of the average size of elements. It is maximum at K_3 (FWHM = = 4700 km) and decreases outwards with increasing $|\Delta\lambda|$. The decrease rate is maximum at $|\Delta\lambda| = 75$ mA (FWHM = 4000 km) and monotonic at K_1 $|\Delta\lambda| \geqq$ $\geqq 0{\cdot}45$ A (FWHM = 2200 km). Corresponding sizes given by Simon and Leighton (1964) and Bappu and Sivaraman (1971) are somewhat larger. This comes from our use of high resolution spectra. The size $\simeq$4000 km accords well with that given by Howard (1962) for the average size of magnetic elements, though the corresponding FWHM for magnetic elements observed by Livingston (1968) is larger.

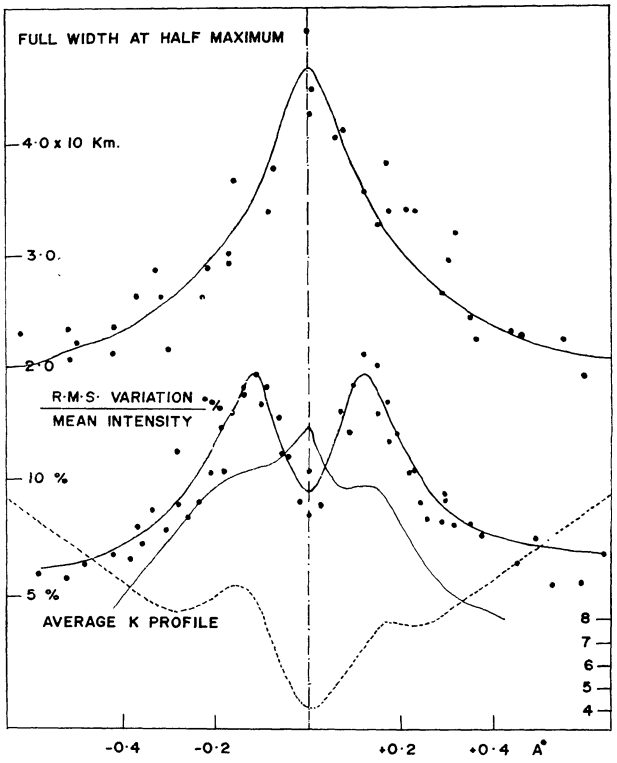

Fig. 2. Wavelength ($\Delta\lambda$) variation of Full Width at Half Maxima (FWHM) and percentage R. M. S. intensity.

Increase in the feature size with height for all types of elements has been shown by Noyes (1967), and Wilson (1970) has discussed the increase with height of the horizontal dimension of the network. The increase in the average size of elements accords well with these observations, though the increase is rather more pronounced at the $K_2 - K_3$ level. The element size does not decrease in K_3, showing that the increase is genuine and not due to the non-LTE effect induced illusion, as discussed by Rybicki (1967).

The sum FWHM's have a lower value than that of intensity and it decreases (4000–2500 km) as the $|\Delta\lambda|$ is increased from 0·08 A to 0·29 A, whereas the difference FWHM is constant (2500 km) over this wavelength range. The DIFF features, though they show an increase in RMS amplitude, remain constant in size as the chromospheric height increases.

Table 1 gives the percentage RMS variations at 0·5 A interval. This has a double-peaked distribution with a minimum at K_3 (RMS = 8·9%) and peaks falling at $|\Delta\lambda| = 0{\cdot}12$ A (RMS = 14·1%). The lower curve in Figure 2 has been obtained by taking a

10 minute time average of RMS variations along the slit from spectra taken with smaller image size (5·5″/mm). The peak at K_3 in it is due to the inclusion of more coarse network boundaries, which due to their large amplitude intensity changes have boosted up the K_3 dispersion.

Table 1

$\Delta\lambda$ A	FWHM km ±250 km	% R. M. S. variation: ±8% uncorrected for seeing	% R. M. S. variation: Corrected for seeing	52× R. M. S. velocity km/sec
0·00	4700	8·5	10·2	
0·05	4300	10·1	12·6	2·36
0·10	3700	13·0	17·5	1·80
0·12		14·1	at R. M. S. Maximum	13·00
0·15	3250	12·5	18·2	28·20
0·20	3000	10·6	16·5	
0·25	2750	8·9	15·0	
0·30	2600	7·7	14·0	
0·35	2450	6·9	13·5	
0·40	2300	6·4	13·6	
0·45	2200	6·2	14·0	
0·50	2150	5·8	13·8	
Mean of intensities				
0·08	3900	11·3		
0·15	3900	11·9		
0·22	3150	10·9		
0·29	2650	9·4		
Difference of intensities				
0·08	2600	12·8		
0·15	2450	12·1		
0·22	2450	9·3		
0·29	2450	7·6		

Macroturbulence velocities calculated on the basis that these RMS variations are caused by the wiggly spectral lines (Reichel, 1953) are of correct order of magnitude, 1−2 km/sec, only in K_3, $0{\cdot}0 \leqq |\Delta\lambda| \leqq 0{\cdot}1$ A, for the velocities to be measured by the method of Evans and Michard (1962). In the rest of the profile, the velocities are higher by an order of magnitude (cf. Table 1), due to the small slope of the line profile. Reichel (1953) observed in spectroheliograms obtained in metallic lines that, on a pure absorption model, the RMS maxima fall at the edge of the Doppler core $\Delta\lambda_m = 3\,\Delta\lambda_D$. This for K line give $\Delta\lambda_D = 0{\cdot}4$ A, corresponding to a microturbulence velocity of 1·75 km/sec for a chromospheric temperature of 15 000 °K.

Figure 3 (see Plate 2) shows the Autocorrelation Functions (ACF) and their power spectra for the intensity, sum and difference series. These are the mean of the three functions that are obtained from the three spectra and the vertical bars in the figure show their internal probable error.

The intensity and the sum ACF's consistently flatten out as the $|\Delta\lambda|$ is decreased corresponding to the increase of average size of elements towards K_3 from either side. Only the $K_3 - K_{2v}$ section the ACF's show roughly a Gaussian core and dispersion wing analogous to that of small scale magnetic field ACF (Livingston, 1968). The K_1 sections, $0{\cdot}25 \leqq |\Delta\lambda| \leqq 0{\cdot}50$ A, show a minor secondary maxima at $L \simeq 6000-7000$ km, indicative of the average separation of the coarse elements.

The power spectra have the wavelength (Lkm) resolution limits, $\pi/10\,000 \leqq 2\pi/L \leqq \pi/170$, defined by the lag interval used and 25 χ^2 degrees of freedom. They show a peak at $\infty > L \geqq 10\,000$ km and decrease sharply to $L \simeq 2000-3000$ km and thereafter decrease slowly through the smaller L's. Rogerson (1955) has found that the K_{232} structural power is large in 75 000 − 25 000 km interval and decreases sharply thereafter.

Wavelength ($\Delta\lambda$) variation of the three parameters defining: R, the relative power in small scale ($L \leqq 2000$ km) features to that in large scale features; a_1, the logarithmic slope of power density with wave number, $K = 2\pi/L$, through 10 000 − 2000 km interval; a_2, the logarithmic slope through small features are shown in Fig. 4.

The relative power, R, in small scale structure is small, 2−8%, and decreases quite sharply through $K_1 - K_2$ and remains almost constant through $K_2 - K_3$. The power structure in K line is substantially different from that of the lower chromospheric lines, such as Mg b, which contain almost equal power in small scale structure (Cannon and Wilson, 1970). The rate of this decrease of power towards small scale structure, a_1, increases sharply through $K_1 - K_2$ and is maximum at K_2R, showing that the coarse mottle features become coarser, i.e., more amorphous, towards the line center and are coarsest at K_2R, though the RMS variations are equal at K_2V and K_2R. These two parameters show that the chromospheric emission in K_{123} does not extend much beyond the K_1 minima. These results are borne out by the frequency sweep spectroheliograms obtained by Title (cf. Zirin, 1966). The sum function power is more concentrated in large size features, whereas the

asymmetric (difference) changes in the line profile show the small scale structure better.

Though the seeing was estimated to be of the order of 1 arc second, the small scale power structure, a_2, does not vary much across the K line.

As regards the profile parameters, there is a regular progression in large scale features becoming less prominent through K_3 minimum position, K_3 minimum intensity, exponential width of K_3 and K_1 (0·4−0·7 A) mean intensity (Fig. 5). A similar progression is observed in K_1-min width, K_2-peak width and K_3 exponential width.

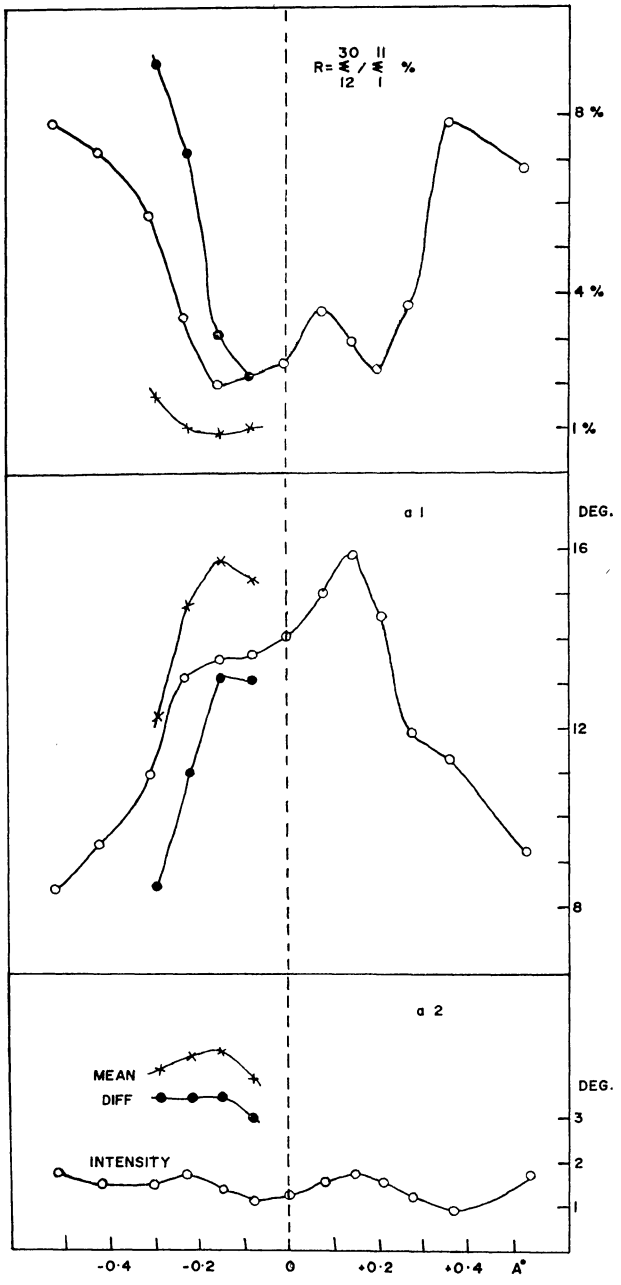

Fig. 4. Wavelength ($\Delta\lambda$) variation of the power spectra parameters: R, the fractional power in small scale ($\leqq$ 3000 km.) features as compared to that at large scale features; 'a_1' and 'a_2', the logarithmic slope with wavenumber in 10 000 through 3000 km features and through less than 3000 km features respectively.

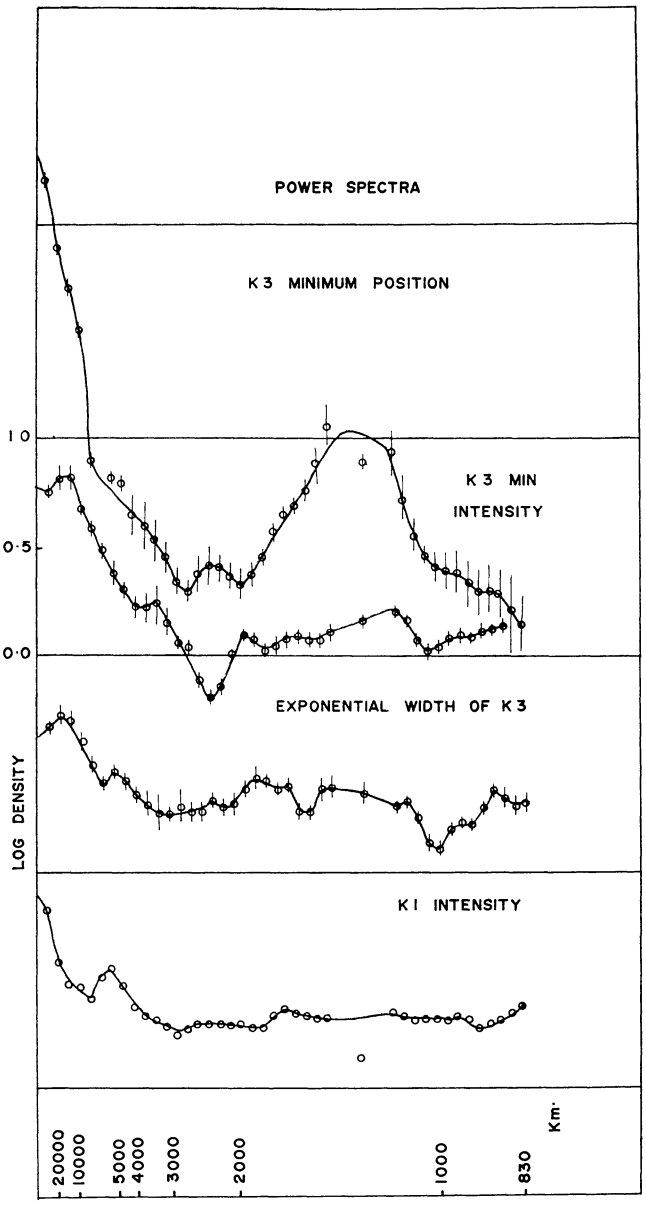

Fig. 5. Power spectra of K_3 minimum position, K_3 minimum intensity, exponential width of K_3, and K_1 (0·300 $\leqq \Delta\lambda \leqq$ 0·700 A) intensity.

Cross correlation studies (Fig. 6) show that significant coherence, >0·5, is observed through large scale structure, 20 000 − 2000 km, in symmetric intensity change: K_1-min intensity/K_2-wing sum (7−18), K_1-min sum/K_2-peak sum (15−17), and K_2-wing sum/K_3-wing sum (16−18), while the difference changes (7−21, 18−21 and 19−21) are poorly related to the overall line brightening and darkening.

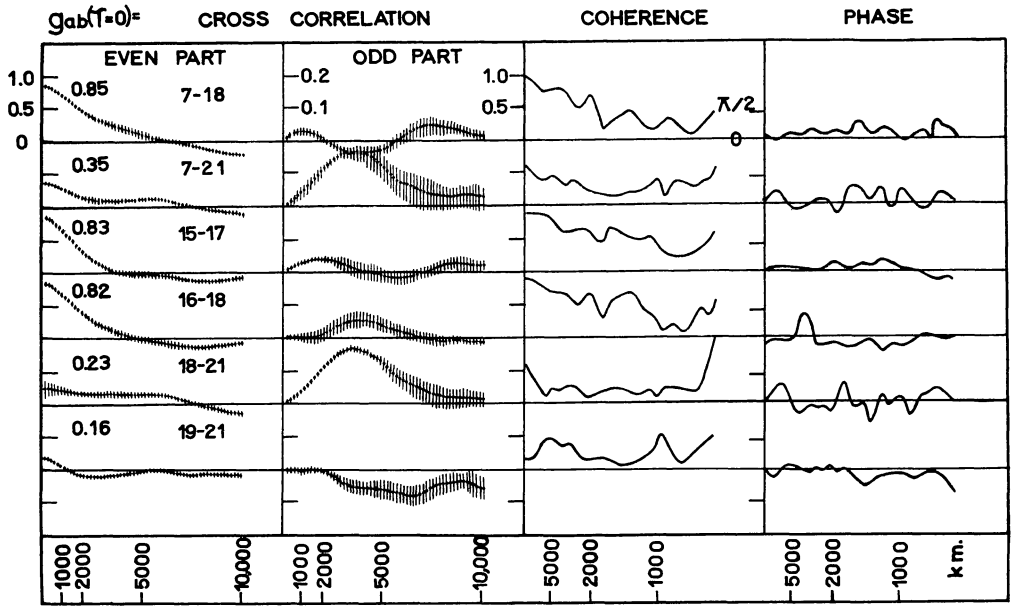

Fig. 6. Cross correlation, even and odd parts, and their coherence and phase spectra for various series: K_3 INTY/K_3-Wing SUM (7—18), K_3 INTY/K_2-peak DIFF (7—21), K_1-min SUM/K_2-peak SUM (15—17), K_2-wing SUM/K_3-wing SUM (16—18), K_3-wing SUM/K_2-peak DIFF (18—21) and K_1-min DIFF/K_2-peak DIFF (19—21).

Discussion

The visibility function, i.e., the RMS variations, has its peak at 0·12 A, which is inwards of the average K_2 peaks at 0·16 A. A combination of both the mechanisms, (1) decrease in K_2 peak separation with increasing intensity (Smiths, 1960), and (2) independent RMS variations of K_2 peaks of $\pm$0·04 A over the quiet sun disk (Pasachoff, 1970), may be invoked to explain this effect. But the K_2 separation shows large power concentrated at large scale features, and K_2 peak separation and K_2 average intensity are poorly related at all the wavelengths (L). This emphasizes the need for a careful separation of these effects with regard to feature size.

One component models for the K line formation have failed to reproduce the observed limb darkening and the observed changes in profile shape towards the limb (Linsky and Avrett, 1970). Two and three component models have been investigated by Beebe and Johnson (1969), Beebe (1971), Wilson (1970) and Cram (1972). They have mainly concentrated on the two aforesaid line profile characteristics and have taken the relative contribution of various components arbitrarily. A more realistic approach would be that these models give a due cognizance to the relative variations in large and small scale features while reproducing the average profiles. In this respect we feel that the network and especially the coarse mottle variations have been under-represented even with regard to the Wilson-Bappu effect, where the coarse structure variations predominate in K_1-width, K_2-width and K_3-width power spectra.

Recently more emphasis has been given to the small scale features (Pasachoff, 1970; Bappu and Sivaraman-1971; Wilson and Evans, 1971; Wilson et al., 1972). We feel that these features are important by themselves, but they are rather superposed over the coarse structure and their contribution to the average line profile is of secondary importance. Coarse mottles have also been found important in the Mg *b* lines (Cannon and Wilson, 1970).

We have found in another program that in the K_1, K_2 and K_3 asymmetric variations, the first two have large power in large scale features whereas the third has almost a flat spectra. Athay (1970) and Cram (1972) have tried to reproduce these features in an isolated form by considering different velocity gradients in the atmosphere, but there again a proper apportionment with respect to scale length should be taken into account to reproduce the average profile and its variability.

Acknowledgments

My sincere thanks are due to Dr. M. C. Pande for helping me and giving valuable suggestions during the data processing and finalizing phase. The data

was collected when I was a Research Scholar at the Kodaikanal Observatory. I am grateful to Dr. M. K. V. Bappu for providing me the spectra and instrumental facilities to trace them.

REFERENCES

Athay, R. G.: 1970, Solar Phys. **11**, 347.
Babcock, H. W., Babcock, H. D.: 1955, Astrophys. J. **121**, 349.
Bappu, M. K. V., Sivaraman, K. R.: 1971, Solar Phys. **17**, 316.
Beebe, H. A.: 1971, Solar Phys. **17**, 304.
Beebe, H. A., Johnson, H. R.: 1969, Solar Phys. **10**, 79.
Cannon, C. J., Wilson, P. R.: 1970, Solar Phys. **14**, 29.
Connes, S.: 1961, Rev. Optique **40**, 45.
Cram, L. E.: 1972, Solar Phys. **22**, 375.
De Jager, C.: 1959, Handbuch Phys. **52**, 80 (Springer-Verlag).
Desland-res, H.: 1910, Ann. Obs. Paris Mendon, **4** (I).
Edmonds, F. N. Jr., Michard, R., Servajean, R.: 1965, Ann. Astrophys. **26**, 368.
Evans, J. W., Michard, R.: 1962, Astrophys. J. **136**, 493.
Hale, G. E., Ellerman, F.: 1903, Publ. Yerkes Obs. **III** (I).
Howard, R.: 1959, Astrophys. J. **130**, 193.
—: 1962, Astrophys. J. **136**, 211.
Jensen, E., Orrall, F. Q.: 1963, Astrophys. J. **138**, 252.
Leighton, R. B.: Astrophys. J. **130**, 366.
Linsky, J. L., Avrett, E. H.: 1970, Publ. Astron. Soc. Pacific **82**, 196.
Livingston, W. C.: 1968, Astrophys. J. **153**, 929.
McMath, R. R., Mohler, O. C., Pierce, A. K., Goldberg, L.: 1956, Astrophys. J. **124**, 1.
Noyes, R. W.: 1967, I. A. U. Symp. **28**, 293.
Pasachoff, J. M.: 1970, Solar Phys. **12**, 202.
—: 1971, Astrophys. J. **164**, 385.
Pasachoff, J. M., Noyes, R. W., Beckers, J. M.: 1968, Solar Phys. **5**, 1.
Reichel, M.: 1953, Z. Astrophys. **33**, 79.
Rogerson, J. B.: 1955, Astrophys. J. **121**, 204.
Rybicki, G. B.: 1967, I. A. U. Symp. **28**, 342.
Simon, G. W., Leighton, R. B.: 1964, Astrophys. J. **140**, 1120.
Smith, E. V. P.: 1960, Astrophys. J. **132**, 202.
Wilson, P. R.: 1970, Solar Phys. **15**, 139.
Wilson, O. C., Bappu, M. K. V.: 1957, Astrophys. J. **125**, 661.
Wilson, P. R., Evans, C. D.: 1971, Solar Phys. **18**, 29.
Wilson, P. R., Rees, D. E., Beckers, J. M., Brown, D. R.: 1972, Solar Phys. **25**, 86.
Zirin, H.: 1966, The Solar Atmosphere (Blaisdell Publ. Co.)

L. M. Punetha
Uttar Pradesh State Observatory
Manora Peak
Naini Tal
263 129, U. P. India

INTENSITY OSCILLATIONS ACROSS THE Ca II K LINE

L. M. Punetha, Uttar Pradesh State Observatory, Naini Tal, India

Received 11 July 1973

Intensities at various wavelengths in the Ca II K line over a 10 minute duration time series spectra have been examined for oscillations. Three components have been observed: 1) large period, $\geqq$1000 second, due to the slowly evolving coarse network; 2) 300 second resonant oscillations; and 3) the 180 second transient recurrent phenomenon. Life history of a typical small scale K_{2v} emission feature is given.

Изменения интенсивности в К линии Ca II

Исследовались колебания яркостей для различных длин волн К линий Ca II по сериям спектров продолжительностью в 10 минут. Наблюдались три компонента: 1) долгопериодический, $\geqq$1000 сек, вызванный медленными изменениями крупных структур; 2) 300 секундные резонансные колебания и 3) 180 секундные переходные рекуррентные явления. Описывается течение типичной мелкомасштабной эмиссии K_{2V}.

Introduction

Quasi-periodic oscillations in K_1, K_2 and K_3 intensities, K_{2V}/K_{2R} intensity ratio and K_{232} profile shape have been observed by Jensen and Orrall (1963). Orrall (1966) has determined velocity oscillations in K_3 by the method of Evans and Michard (1962).

The consistency of these measurements, that they represent velocity oscillations, have been questioned by Pasachoff (1970), who found that most of the chromospheric emission features have single peaked asymmetric profile. Since then the coexistence of single peaked, double peaked and no K_2 peak profile features have been shown by Wilson and Evans (1971), Bappu and Sivaraman (1971) and Liu and Smith (1972).

Wilson and Evans (1971) and Wilson et al. (1972) have shown how the single peaked features evolve into double peaked features in few tens of seconds,